# Organotin-Drug Interactions. Organotin Adducts of Lornoxicam, Synthesis and Characterisation of the First Complexes of Lornoxicam

**Angeliki Galani,[a] Mavroudis A. Demertzis,[a] Maciej Kubicki,[b] and Dimitra Kovala-Demertzi*[a]**

**Keywords:** Antitumour agents / Tin / Supramolecular chemistry / Drug delivery

The synthesis and spectral characterisation of novel organotin complexes [$SnMe_2$(lorn)] (**1**) and [S*n*$Bu_2$(lorn)] (**2**) of the potent and widely used anti-inflammatory drug lornoxicam, $H_2$lorn, are reported. Crystal structure determinations of complexes**1** and **2** showed that the ligand is doubly deprotonated at the oxygen and amide nitrogen atoms and is coordinated to the $SnR_2$ fragment via four- and six-membered chelate rings. The monomers of **1** are linked through intermolecular hydrogen bonds of C–H--O type and through C–H–π intermolecular interactions. There are two similar molecules in the asymmetric unit of **2**. The dimers of **2** are arranged in polymers with a stacking of alternate parallel chains and are linked through intermolecular hydrogen bonds of C–H--O type, and through C–H–π intermolecular interactions. An extended network of Sn–O–Sn, C–H--O and C–H--π contacts lead to aggregation and a supramolecular assembly.



## Introduction

Lornoxicam (6-chloro-4-hydroxy-2-methyl- 2-pyridyl-2*H*-thieno[2,3-*e*]-1,2-thiazine-3- amide-1,1-dioxide) is a new non-steroidal antiflammatory drug (NSAID) with marked analgesic properties that chemically differs from tenoxicam by the presence of a single chloro-substituent in the 8-position.[1] Lornoxicam's principal mode of action is the inhibition of the enzyme cyclooxygenase and thus of prostaglandin synthesis from arachidonic acid.[2] It does not cause shunting of arachidonic acid to the lipoxygenase cascade, and therefore does not increase production of leukotrienes. In vitro experiments have demonstrated that lornoxicam is more than 100 times more potent than tenoxicam and 40 times more potent than piroxicam in its ability to inhibit cyclooxygenase.[1,2] Lornoxicam is a yellow crystalline substance with a p$K$ of 4.7 and a partition coefficient of 1.8 (determined in octanol−phosphate buffer, pH 7.4). The acid−base behaviour of lornoxicam has also been studied and the apparent p$K_a$-values reported.[3]

Organotin(IV) compounds are important and have received increasing attention in recent years, not only because of their intrinsic interest, but also owing to the importance of tin-based anti-tumour drugs. Some examples find wide applications as catalysts and stabilizers, and certain derivatives are used as biocides, as antifouling agents and for wood preservation. Recent tests on their anti-tumour activity have revealed that several diorganotin adducts, as well as triorganotin species, show potential as antineoplastic and antituberculosis agents.[4,5]

We are interested in the coordination chemistry and anti-inflammatory properties of non-steroidal anti-inflammatory drugs with transition[6] and non-transition metal[7] ions, and report here the interaction of $SnR_2O$ (R is methyl or butyl) with lornoxicam ($H_2$lorn) and the crystal structure of the complexes [$SnMe_2$(lorn)] and [S*n*$Bu_2$(lorn)]. These are the first reported structures of a lornoxicam complex.

## Results and Discussion

### Molecular Structures

The molecular structures of complexes **1** and **2**, along with the atom numbering scheme, are shown in Figure 1 and Figure 2 and crystal data are given in Table 1, together with refinement details. Bond lengths and angles are given in Table 2. Complexes **1** and **2** have a 1:1 Sn/lorn stoichiometry and the doubly deprotonated ligand, lorn, is coordinated as a tridentate ligand via the enolic oxygen O(4) and the amide N(31) and pyridyl N(1′) nitrogen atoms. Two carbon atoms complete the fivefold coordination at the diorganotin(IV) fragments. There are two similar molecules in the asymmetric unit of **2**.

Analysis of the shape-determining angles using the approach of Reedijk and co-workers[8] yields $\tau[(\alpha-\beta)/60]$ val-

[a] Inorganic and Analytical Chemistry, Department of Chemistry, University of Ioannina,
45100 Ioannina, Greece
E-mail: dkovala@cc.uoi.gr
[b] Department of Chemistry, A. Mickiewicz, University, ul. Grunwaldzka 6, 60−78 Poznan, Poland

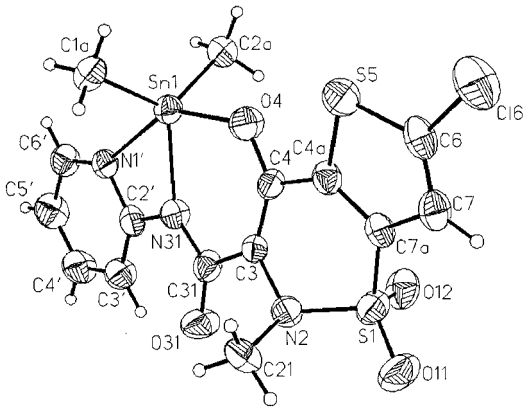


Figure 1. ORTEP representation of **1** with the atom numbering scheme.

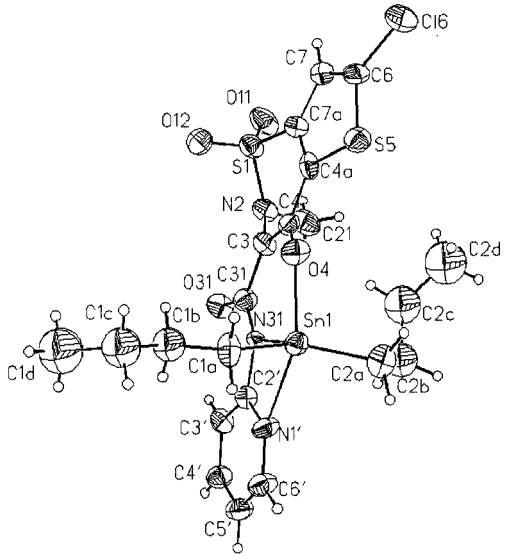


Figure 2. ORTEP representation of **2** with the atom numbering scheme.

ues of 0.01 for both tin centres, Sn(1a) and Sn(1b) for **2**, and 0.29 for **1** ($\tau$ = 0.0 and 1.0 for *sp* and *tbp* geometries respectively). The metal coordination geometry is therefore described as square pyramidal with N(31) occupying the apical positions. The donors N(31) are chosen as apices by the simple criterion that neither should be any of the four donor atoms that define the two largest angles, α and β. The coordinated ligand is composed of five rings and the donor atoms NNO are included in three rings, one heterocyclic and two chelates. The heterocyclic ring (I) is planar, the largest deviation from the mean plane being 0.016(6) for C(2′) for **1** and 0.008(12)° for C(5′A) for molecule (1) and 0.015(11) for C(3′B) for molecule (2), respectively, for complex **2**. For **1** the dihedral angles between the planes of the rings I and II, II and III, and I and III are 3.4(3), 3.8(2) and 6.9(2), respectively. For **2** the dihedral angles between the planes of the rings I and II, II and III, and I and III are 0.8(5), 6.1(4) and 6.8(4) for the first molecule Sn(1a), and 2.7(5), 5.2(4) and 7.1(4) for the second molecule Sn(1b), indicating that the ligand as a whole deviates from planarity, the largest deviations arising from the expected puckering of the sulfonamide rings which contain the pyramidal saturated N atoms. The C(31)−O(31) bond lengths indicate strongly that these bonds are ketonic − also supported by the coplanarity of the three bonds to C(31). The di-anionic, tridentate ligand has an *EZZ* configuration about the bonds C(2′)−N(31), N(31)−C(31) and C(31)−C(3) for **1** and **2**. The *EZZ* configuration differs from the *ZZZ* isomer only by a 180° rotation of the pyridyl ring. The deprotonation of amide nitrogen is being one of the principal effects, which favour *EZZ* configuration.

Table 1. Crystal data, data collection and structure refinement

| Compound | **1** | **2** |
|---|---|---|
| Empirical formula | $C_{15}H_{14}ClO_4N_3S_2Sn$ | $C_{21}H_{26}ClN_3S_2Sn$ |
| Molecular mass | 518.55 | 602.71 |
| Crystal system | monoclinic | triclinic |
| Space group | $P2_1$ | $P\bar{1}$ |
| *a* (Å) | 9.0172(13) | 12.413(2) |
| *b* (Å) | 11.797(2) | 13.272(2) |
| *c* (Å) | 9.2567(17) | 17.705(2) |
| α, β, γ (°) | 90 108.089(16) 90 | 78.058(12) 77.058(12) 63.903(16) |
| *V* (Å$^3$) | 936.0(2) | 2533.1(6) |
| Z | 2 | 4 |
| $D_x$ (g cm$^{-3}$) | 1.84 | 1.58 |
| *F*(000) | 512 | 1216 |
| μ (mm$^{-1}$) | 1.76 | 1.31 |
| Crystal size (mm) | 0.40 × 0.25 × 0.10 | 0.30 × 0.20 × 0.150 |
| Θ Range (°) | 3.8−25 | 3.5−26 |
| *hkl* Range | $-10 \le h \le 10$<br>$-14 \le k \le 12$<br>$-11 \le l \le 11$ | $-14 \le h \le 14$<br>$-15 \le k \le 16$<br>$-21 \le l \le 21$ |
| Reflections: | | |
| collected | 7749 | 12229 |
| unique ($R_{int}$) | 2512 (0.040) | 7688 (0.047) |
| Number of parameters | 235 | 505 |
| Weighting scheme: | | |
| A | 0.01 | 0.137 |
| B | 0.7 | 7.996 |
| Extinction parameter *k* | 0.00091(10) | |
| *R*(*F*) | 0.026 | 0.067 |
| *wR*($F^2$) | 0.049 | 0.169 |
| Goodness of fit | 1.14 | 1.02 |
| max/min Δρ (e·Å$^{-3}$) | 0.92/−0.37 | 2.66/−1.11 |

Molecules of **2** are joined into dimers in a head-to-tail fashion by intermolecular bonds between tin and the neighbouring ketonic oxygen atom, with distances of Sn(1a)--O(31B)$^i$ 2.954 (2) and Sn(1b)--O(31A)$^i$ 2.971 (2). Intermolecular distances for Sn--O of 2.61−3.02 Å have been confidently reported for intramolecular bonds, indicating Sn−O bonding here.[9b] For **2** the dimers of Sn(1a) and Sn(1b) are arranged in polymers with a stacking of alternate parallel chains. The dimers of Sn(1a) and Sn(1b) are linked through intermolecular hydrogen bonds of the C−H--O type,[9a] O(12B)l···H22A−C(2AA). Inter- and intra- C−H-π molecular interactions[9b] and intra- and intermolecular hydrogen bonds stabilize this structure. For **1** the distance between

  

Table 2. Selected bond lengths [Å] and angles [°] for **1** and **2**

| | **1** | **2a** | **2b** |
|---|---|---|---|
| Sn(1)−C(1A) | 2.102(6) | 2.123(9) | 2.118(9) |
| Sn(1)−C(2A) | 2.112(5) | 2.104(11) | 2.113(11) |
| Sn(1)−N(31) | 2.120(5) | 2.133(8) | 2.140(8) |
| Sn(1)−N(1′) | 2.400(4) | 2.407(8) | 2.391(7) |
| Sn(1)−O(4) | 2.094(3) | 2.113(6) | 2.108(6) |
| S(1)−O(11) | 1.422(4) | 1.435(8) | 1.444(8) |
| S(1)−O(12) | 1.440(4) | 1.413(8) | 1.419(8) |
| S(1)−N(2) | 1.624(5) | 1.631(8) | 1.620(9) |
| S(1)−C(7A) | 1.740(5) | 1.735(10) | 1.746(10) |
| C(4)−O(4) | 1.315(6) | 1.338(10) | 1.318(10) |
| C(4A)−S(5) | 1.718(5) | 1.729(9) | 1.731(9 |
| S(5)−C(6) | 1.719(5) | 1.738(11) | 1.714(10) |
| C(31)−O(31) | 1.221(6) | 1.247(11) | 1.249(11) |
| C(31)−N(31) | 1.365(7) | 1.374(11) | 1.384(12) |
| N(31)−C(2′) | 1.394(6) | 1.411(11) | 1.389(12) |
| N(1′)−C(6′) | 1.335(6) | 1.329(12) | 1.357(12) |
| N(1′)−C(2′) | 1.351(6) | 1.330(11) | 1.348(12) |
| | | | |
| O(4)−Sn(1)−C(1A) | 97.1(2) | 96.1(4) | 97.0(4) |
| O(4)−Sn(1)−C(2A) | 97.19(17) | 101.3(4) | 99.7(4) |
| C(1A)−Sn(1)−C(2A) | 126.1(2) | 142.1(4) | 140.6(4) |
| O(4)−Sn(1)−N(31) | 85.09(15) | 83.3(2) | 83.5(2) |
| C(1A)−Sn(1)−N(31) | 116.2(2) | 104.6(3) | 105.5(3) |
| C(2A)−Sn(1)−N(31) | 116.63(19) | 110.6(4) | 111.7(4) |
| O(4)−Sn(1)−N(1′) | 143.79(13) | 141.4(2) | 141.4(3) |
| C(1A)−Sn(1)−N(1′) | 100.5(2) | 92.3(4) | 92.5(4) |
| C(2A)−Sn(1)−N(1′) | 97.56(17) | 94.6(4) | 96.2(4) |
| N(31)−Sn(1)−N(1′) | 58.75(15) | 58.2(3) | 57.9(3) |
| N(31)−C(31)−C(3) | 115.8(5) | 114.1(7) | 116.0(8) |
| N(31)−C(31)−O(31) | 122.8(5) | 126.2(8) | 124.6(9) |
| O(31)−C(31)−C(3) | 121.4(5) | 119.6(8) | 119.4(8) |

Sn(1) and the neighbouring ketonic oxygen atom is 3.562(4), and the monomers of Sn(1) are linked through intermolecular hydrogen bonds of C−H--O type,[9a] O(12)axial···H6′−C(6′), O(11)eq···H13A−C(1A) and O(31)···H23A−C(2A) (Figure 3). Further, C−H−π interactions[9a] and intramolecular hydrogen bonds stabilize the structure. Although the numerous contacts, of many different types, are remarkable, the interactions themselves are consistent with known guidelines for hydrogen bond formation.[9c] In these two cases molecular recognition of the hydrogen bonds and intermolecular contacts lead to aggregation and a supramolecular assembly. These interactions and other close approaches of the type C−H--π, and some intermolecular interactions are listed in Table 3.

The negative charge on the atoms in a molecule with several donor centres can be used to study its formation of a donor−acceptor bond with a metal. In $H_2$lorn the four oxygen atoms exhibit the maximum electron density and negative charge. The highest effective charge and the highest electron density values for the four oxygen atoms and for the pyridyl and imine nitrogen in **1** and **2** evidently show strong electron-donor properties and could rationalize the coordination scheme and the extended network of inter-, intra- hydrogen, and non-hydrogen bonding. The optimised geometry in the gas phase for $H_2$lorn the total dipole moment and the enthalpy of formation of neutral, $H_2$lorn, and double deprotonated lornoxicam, lorn, in the gas state are shown in Figure 4.

## Spectral and Electrochemical Characterisation

### *Infrared Spectroscopy*

The ligand, $H_2$lorn, shows a broad absorption band centred at ca. 3500 and 3400 $cm^{-1}$ that is characteristic of an O−H stretching vibration. The band at 3067 $cm^{-1}$ for lornoxicam is attributed to the N−H stretching vibration. The low frequency of these two bands may be explained by inter- and intramolecular hydrogen bonds involving the nitrogen and two oxygen atoms of the secondary amide group.[11a] The sharp bands observed at 1647, 1619 $cm^{-1}$ and the band at 1596 $cm^{-1}$ in lornoxicam are assigned to the carbonyl $\nu$(C=O) and the $\nu$(C=N) vibrations of the secondary amide group −CO−NH−.[11] The $\nu$(C=O) and the $\nu$(C=N) bands are at lower frequencies in the complexes, at 1619, 1591 and 1567 $cm^{-1}$ for **1** and at 1600, 1599, 1578 and 1549 $cm^{-1}$ for **2**. For compounds **1** and **2**, bands assignable to $\nu_{asym}$ and $\nu_{sym}$ (Sn−$C_2$) are observed at 550, 473 and 551, 475 $cm^{-1}$ respectively, indicating a non-linear Sn−$C_2$ moiety. The bands at 265 and 268 $cm^{-1}$ are assigned to the $\nu$(Sn−$N_{pyr}$) stretching mode for **1** and **2** respectively; and those at 221 and 215 $cm^{-1}$ for **1**, and at 224 and 211 $cm^{-1}$ for **2**, are assigned to $\nu$(Sn−O) stretching modes.[7,11]

### *NMR Spectroscopy*

$^1$H and $^{13}$C NMR spectra were recorded for lornoxicam, **1** and **2**. Peak assignments were based on literature reports.[6,7] The main differences between the $^1$H NMR spectrum of the free $H_2$lorn and the complexes are the disappearance of the downfield OH and NH signals. These changes confirm that loss of both hydrogens and metallation occurs, and that the structure of the complexes in the solid state persists in $(CD_3)_2SO$ or $CDCl_3$ solutions. The appearance of the OH peak downfield at $\delta$ = 14.02 ppm in $CDCl_3$ for $H_2$lorn indicates that OH is hydrogen-bonded. In complexes **1** and **2** deshielding of protons H6′, H3′ and the corresponding carbon atoms C(6′), C(3′) is observed, which should be related to the electrophilicity of the tin. A σ-charge donation from the N(1′)-donor to the tin centre removes electron density from the ligand and produces this deshielding, which will attenuate at positions remote from the metal. The upfield shift observed for H4′, H5′ and the corresponding carbon atom C(4′), C(5′) *meta* and *para* to the tin centre could be due to the flow of charge from the tin into the aromatic ring (π-back donation).[7] The signals corresponding to the imino and hydroxyl groups disappear upon interaction with the metal, indicating deprotonation of these atoms and possible coordination to the tin atom. A tridentate coordination via the enolic oxygen, the amide and the pyridyl nitrogen atoms has been recently observed for the first time in a similar complex of piroxicam, $[Bu_2Sn(Pir)]_n$, and tenoxicam, $[Bu_2Sn(ten)]_n$, where the ligand exists also in its doubly deprotonated form.[7] These

  

Table 3. Inter-hydrogen bonding, non-hydrogen, π−π and C−H-π interactions

| Compound **1** | | | | |
|---|---|---|---|---|
| D−H···A | *d*(D−H) | *d*(H···A) | *d*(D···A) | <(DHA) |
| C(2A)−H(2A3)···O(31)$^{i}$ | 0.96 | 2.57 | 3.380(7) | 142.2 |
| C(6′)−H(6′)···O(12)$^{i}$ | 0.93 | 2.39 | 3.072(7) | 130.2 |
| C(1A)−H(1A3)···O(11)$^{ii}$ | 0.96 | 2.51 | 3.315(8) | 141.7 |
| C(1A)−H(1A3)···Cl(6)$^{iii}$ | 0.96 | 3.02 | 3.821(7) | 142.1 |
| Cg(I) (ρ) Cg(J)[a] | Cg−Cg[b] | β≅[c] | CgI-Perp[d] | CgJ-Perp[e] |
| Cg(5) (ρ) Cg(2)$^{iii}$ | 3.798 | 15.05 | 3.668 | 3.461 |
| | | H···Cg | X···Cg | C−H···Cg |
| C(1A) −H(11A) → Cg(3)$^{i}$ | | 3.382 | 92.98 | 3.563 |
| C(1A) −H(12A) → Cg(3)$^{i}$ | | 2.882 | 128.81 | 3.563 |
| C(2A) −H(21A) → Cg(2)$^{iv}$ | | 3.344 | 106.61 | 3.734 |
| Compound **2** | | | | |
| D−H···A[f] | *d*(D−H) | *d*(H···A) | *d*(D···A) | <(DHA) |
| C(21A)−H(21B)···Cl(6B)$^{v}$ | 0.96 | 2.93 | 3.815(12) | 154 |
| C(1AB)−H(1A4)···Cl(6B)$^{v}$ | 0.97 | 2.94 | 3.835(11) | 154 |
| C(21B)−H(21E)···Cl(6A)$^{vi}$ | 0.96 | 2.95 | 3.850(12) | 156 |
| C(2AA)−H(2A2)···O(12B)$^{vii}$ | 0.97 | 2.42 | 3.303(15) | 152 |
| Sn(1A)···--O(31B)$^{vii}$ | | | 2.953(7) | |
| Sn(1B)···--O(31A)$^{viii}$ | | | 2.971(7) | |

[a] Where Cg(2), Cg(3) and Cg(5) are referred to the centroids S(5)−C(4A)−C(7A)−C(7)−C(6), O(4)−C(4)−C(3)−C(31)−N(31) and N(1′)−C(2′)−C(3′)−C(4′)−C(5′)−C(6′) for **1** respectively. [b] Cg−Cg is the distance between ring centroids. [c] β is the angle Cg(I)−Cg(J) or Cg(i)−Me vector and normal to plane I (°). [d] CgI-Perp is the perpendicular distance of Cg(I) on ring J. [e] CgJ-Perp is the perpendicular distance of Cg(J) on ring I. [f] D is donor and A is acceptor; symmetry transformations used to generate equivalent atoms, (i) $2-x$, $-1/2+y$, $2-z$; (ii) $-x+2$,$y-1/2$, $-z+1$; (iii) $x-1$, $y$, $z$; (iv) $x$, $y$ $1+z$; (v) $1-x$, $2-y$, $-z$; (vi) $1-x$, $2-y$, $-z$; (vii) $1+x$, $-1+y$, $z$; (viii) $-1+x$, $1+y$, $z$.

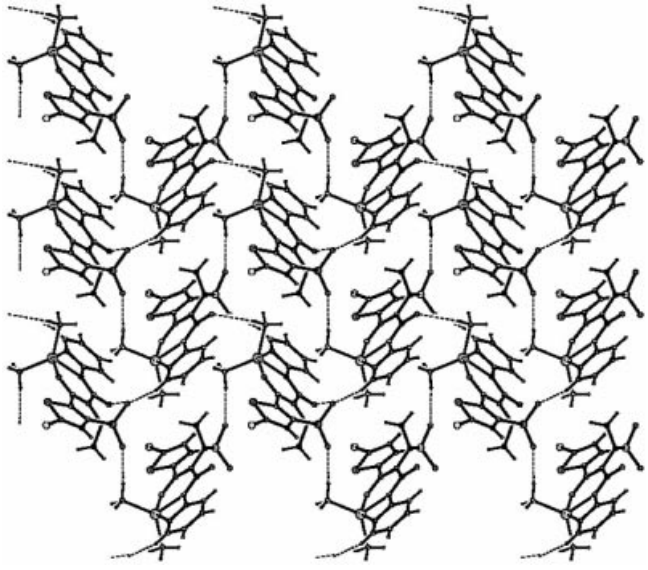

Figure 3. Packing diagram of the complex **1** viewed along the *a* axis of the unit cell, showing intermolecular interactions.

conclusions are confirmed by the $^{13}C$ NMR spectrum where the signal corresponding to C(4) disappears while the signals to C(3) and C(5) show downfield shift. The bond development of the N(1′) atom with the metal leads to a downfield shift by 6.0 ppm of the C(6′) and C(3′) while the C(4′) and C(5′) shift in the opposite direction by 2.0 ppm.

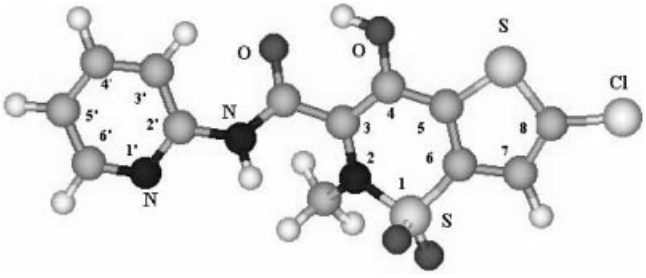


Figure 4. Fully AM1-optimised geometry of the neutral lornoxicam ($\Delta H_f$ = −48.28 kcal mol$^{-1}$; dipole moment = 3.98 Debye) in the gas state (Hyperchem 6.0[10]).

### *Electronic Spectroscopy*

The electronic spectrum of $H_2$lorn in DMF solution exhibits two broad bands at ca. 398 and 273 nm. The band at 398 nm is assigned to a π → π* and that at 273 nm to a π → π* transition. The very broad band at ca. 400 nm is assignable to a HOMO → LUMO transition. The HOMO orbital (−10.972 eV) is composed of $p_z$ orbitals from Cl 6% (+), C(8)$p_z$ 12% (−), C(5)$p_z$ 12% (+), C(6)$p_z$ 11% (+), C(7)$p_z$ 10% (−), C(4)$p_z$ 6% (−), C(3)$p_z$ 18% (−), N(2)$p_z$ 8% (+) and the LUMO orbital (−9.261) is composed of $p_z$ orbitals from C(6)$p_z$ 5% (+), C(2′)$p_z$ 11% (−), C(4′)$p_z$ 14%

  

(+), C(6′)$p_z$ 6% (−), N(1′)$p_z$ 11% (+), C(4) $p_z$ 10% (−),C(10) $p_z$ 17% (+). The HOMO orbital is π-centred on the sulfonamide and thiazine groups and the LUMO orbital is mainly π-centred on the pyridyl ring. $H_2$lorn and complexes **1** and **2** were studied by the extended-Hückel method using the CACAO PC Beta-Version 5.0 package geometry.[12] The molecular geometry was established by using the crystallographic coordinates of the complexes **1** and **2** and for $H_2$lorn by using the fully optimised in the gas state. The broad band centred at 376 and 373 nm respectively for **1** and **2** is assigned to a HOMO → LUMO transition. The extended-Hückel calculation using the crystallographic coordinates of **1** gives the following results: the HOMO orbital (−11.354eV) is composed of $p_z$ orbitals from C(l6)$p_z$ 5%(−), C(3)$p_z$ 7%(+), C(6)$p_z$ 9%(+), C(7)$p_z$ 7%(+), C(7a)$p_z$ 7%(−) and of $p_y$ from C(3)$p_y$ 11%(+); the LUMO orbital (−9.294 eV) is composed of $p_y$ from C(4)$p_y$ 10%(−), C(31)$p_y$ 11%(+) and $p_z$ orbitals from C(4) $p_z$ 7%(−), C(7a)$p_z$ 6%(+), C(31)$p_z$ 9%(+). The extended-Hückel calculation using the crystallographic coordinates of **2** gives the following results: the HOMO for (−11.334 eV) is composed of $p_x$ orbitals from C(3)$p_x$ 10%(−), C(4a)$p_x$ 6%(+), C(6)$p_x$ 5%(−), C(7a)$p_x$ 5%(+), C(7)$p_x$ 5%(−) of $p_z$ C(3)$p_z$ 8%(+), C(4a)$p_z$ 11%(−), C(6)$p_z$ 8%(+), C(7a)$p_z$ 5%(−), C(7)$p_z$ 6%(+); the LUMO (−9.322 eV) is composed of $p_x$ from C(4)$p_x$ 10%(−), C(7a)$p_x$ 4%(+), C(31)$p_x$ 13%(+) and $p_z$ orbitals from C(4)$p_z$ 10%(+), C(6)$p_z$ 3%(+), C(7a)$p_z$ 5%(−), C(31)$p_z$ 14%(−). The HOMO energy is isolated, suggesting that the assignment of the lowest energy electronic transition can be assigned to the computed HOMO−LUMO. Also, the similarity of the HOMO−LUMO gap from the calculations (2.060 and 2.012 eV for **1** and for **2** respectively) is reflected in the similarity of the first absorption band energy at ca. 375 nm in the complexes.

The HOMO−$n$ ($n$ = 1−6) levels for **1** are similar in energy, and are more stabilized (by ca. 1.4 eV) relative to the HOMO. The molecular orbital HOMO−6 has components of $p_y$ (7%) and $p_z$ (8%) from Sn, and p atomic orbitals from C(1a) and C(2a). Also, the molecular orbital HOMO-4 for **2** is stabilized by 1.01 eV relative to the HOMO and has components of $p_x$ 6%(−) from Sn and p atomic orbitals from N(1′), C(3′), C(4′), C(5)′ and C(1b) This is consistent with a back donation from the metal to the π* orbitals of the ligand moieties.[13] The broad band at 292 and 295 nm for **1** and **2** is assigned to a combination of π → π* and M → L transitions. It has been found that the interaction of C−Sn σ orbitals and neighbouring p-type orbitals increases the HOMO level, which in turn favours electron transfer. Such σ-π interaction, σ−n and σ−σ interactions enjoy versatile applications in the field of electron transfer.[14]

### *Electrochemical Measurements*

The ability of the complexes to either gain or to lose electrons was studied in anhydrous DMF solution by cyclic voltammetry. The ligand exhibits irreversible reduction peaks at −1.143 and −1.543 V. Irreversible reductions are seen at −0.764 and −1.267 V for **1**, and at −1.135 and 1.792 V for **2**. The electrochemical data suggest that the reduction of **1** and **2** might be regarded as being more or less centred on the ligand system. The electron transfers from the platinum cathode and is directed to the π* LUMO orbital. The reduction potential of **1** is less negative, while that of **2 is** more negative for the corresponding ligand and decreases in the order **1** < **$H_2$lorn** < **2**, indicating that the reduction process is more easily accomplished for 1 than for either free **$H_2$lorn** or **2**. The oxidation wave for **$H_2$lorn** is observed at +0.610 and that for **1** and **2** at 0.483 and 0.842 V, respectively. The oxidation is also associated with a ligand-based process and oxidized products are formed. The oxidation potentials of **1**, **2**, and **$H_2$lorn** increase in the order **2** > **$H_2$lorn** > **1**. Thus, both the reduction and oxidation processes in complex **1** are more easily accomplished than in either **2** or the parent drug. However, in the range from +1.5 to −2.5 V additional peaks are observed.

## Experimental Section

All the chemicals used were of high purity and purchased from Fluka, Merck and Aldrich. Solvents were purified and dried according to standard procedures. Tenoxicam was a gift from "NYCOMED" NYCOMED DENMARK A/S and was recrystallised twice from ethanol. Elemental analyses were performed on a Carlo Erba EA (model 1108). Infrared and far-infrared spectra were obtained in KBr or polyethylene discs on a Perkin−Elmer Spectrum JX FT-IR spectrophotometer. A Jasco UV/Vis/NIR V 570 series spectrophotometer was used to obtain the electronic absorption spectra. $^1$H (250.13 MHz) and $^{13}$C (62.90 MHz) NMR spectra were recorded with a Bruker AMX-400 spectrometer at room temperature and referenced to DMSO or $CHCl_3$. UV spectra were recorded on a JASCO V-570 spectrophotometer. Electrochemical measurements were made using an AUTOLAB PGSTAT30 potentiostat with a platinum microsphere as working electrode, a platinum wire auxiliary electrode and an Ag/AgCl reference electrode in a three-electrode configuration. Ferrocene was added at the end of each experiment and used as an internal standard. All potentials are reported relative to an Ag/AgCl reference electrode and ferrocenium/ferrocene ($Fe^+$/Fc, $E_{1/2}$ = 0.173 V in DMF). Experiments were carried out on $1 \times 10^{-3}$ M solutions of complex, under a nitrogen atmosphere, with $Et_4NClO_4$ (0.1 M) as supporting electrolyte (scan rate 100 mV $s^{-1}$).

### *Preparations*

**[$SnMe_2$(lorn)]$_n$ (1):** $SnMe_2O$ (0.066 g, 0.4 mmol) was added to a solution of lornoxicam ($H_2$lorn) (0.150 g, 0.4 mmol) in benzene (25 $cm^3$) and the reaction mixture was refluxed for 7 h under a Dean−Stark trap. The resultant clear solution was rotary evaporated under vacuum to a small volume, chilled and triturated with diethyl ether to give a yellow solid that was redissolved (suspended) in dry diethyl ether and the same procedure was repeated twice. The final yellow product was filtered off and dried in *vacuo* over silica gel. (**1**) m.p. 260−262 °C; Yield 90%. $C_{15}H_{14}ClN_3O_4S_2Sn$ (518.6): calcd. C 34.31, H 2.70, N 8.10, S 9.92; found C 34.88, H 2.65, N 8.30, S 10.3. Crystals of **1** suitable for X-ray analysis were obtained by slow evaporation of a fresh EtOEt/$CH_2Cl_2$ solution.

**[Sn(*n*-$C_4H_9$)$_2$(Hlorn)$_2$] (2):** Sn(*n*-$C_4H_9$)$_2$O (0.099 g, 0.4 mmol) was added to a solution of lornoxicam ($H_2$lorn) (0.150 g, 0.4 mmol) in

  

benzene (25 $cm^3$) and the reaction mixture was refluxed for 27 h under a Dean−Stark trap. The resultant clear solution was rotary evaporated under vacuum to a small volume, chilled and triturated with hexane to give a yellow solid that was redissolved (suspended) in hexane and the same procedure was repeated twice. The final light yellow product was filtered off and dried in *vacuo* over silica gel (**1**). M.p. 174−176 °C; Yield 66%. $C_{21}H_{26}ClN_3O_4S_2Sn$ (602.7): calcd. C 41.84, H 4.32, N: 6.97, S 10.65; found C 42.10, H 4.56, N 6.65, S 10.38. Crystals of **2** suitable for X-ray analysis were obtained by slow evaporation of a fresh $C_6H_{12}/C_6H_6$ solution.

### Crystal Structure Determination of Complexes 1 and 2

X-ray diffraction data were collected on a KUMA KM4CCD κ-geometry diffractometer with a CCD detector,[15] by using graphite-filtered Mo-$K_\alpha$ radiation (λ = 0.71073 Å). The unit cell dimensions were calculated from the least-squares fit of 2163 (**1**) and 1450 (**2**) most intense reflections from the whole experiment. Relevant crystallographic data, together with data collection and structure refinement details, are listed in Table 1. The measurements were performed in six separate runs, four runs consisted of 133 frames, and two of 125 frames (ω width of each frame was 0.75°). The θ, κ and angles for the runs were chosen so as to cover the appropriate part of the Ewald sphere. Two reference frames were measured after every 50 frames of experiment; neither the geometry nor the intensity of the reflections in these frames changed significantly during the data collection. Intensity data were corrected for Lorentz and polarisation effects and converted into $F^2$'s. These data were corrected for absorption and averaged with respect to the point group symmetry with SORTAV program.[15b] The structures were solved with SHELXS-97,[16] and SHELXL-97[16] was used for full-matrix least-squares refinement. The function $\Sigma w(0.5F_o1/2^2 - 0.5F_c1/2^2)^2$ was minimised, with $w^{-1} = [\sigma^2(F_o)^2 + A{\cdot}P^2 + B{\cdot}P]$ (where $P$ = [max. ($F_o^2$, 0) + $2F_c^2$]/3). Final values for A and B are listed in Table 1. In **1** all the non-hydrogen atoms were refined anisotropically, in **2** − due to the large thermal motion of the butyl groups − only the first atoms of these groups (connected to Sn) were refined anisotropically, while the other three atoms from each butyl groups were refined isotropically, with fixed values for $U_{iso}$. The (relatively weak) constrains were also applied to the geometry of these groups. The attempts to resolve the apparent disorder of butyl groups were not successful. In both structures, hydrogen atoms were placed in calculated positions and refined as "riding mode", i.e. they followed the movements of their carrier atoms. The isotropic displacement parameters for hydrogen atoms were calculated as 1.2 times equivalent displacement parameters for respective carrier non-hydrogen atoms.

### Calculations

A computational study with a AM1 parameterization scheme utilizing the Steepest Descent algorithm, as implemented in the HYPERCHEM 6.0 program, was used to investigate the prevailing isomer of free $H_2$lorn in the gas phase.[10] $H_2$lorn and the complexes **1** and **2** were studied by the extended-Hückel method using the CACAO PC Beta-Version 5.0 package geometry.[12] The molecular geometry was established by using the crystallographic coordinates of complexes **1** and **2** and for $H_2$lorn by using the fully optimised in the gas state.[12]

### Supplementary Material

CCDC-193499 for **1** and CCDC-193498 for **2** contain the supplementary crystallographic data for this paper. These data can be obtained free of charge at www.ccdc.cam.ac.uk/conts/retrieving.html [or from the Cambridge Crystallographic Data Centre, 12, Union Road, Cambridge CB2 1EZ, UK; Fax: (internat.) +44-1223/336-033; E-mail: deposit@ccdc.cam.ac.uk].

## Acknowledgments

We thank NYCOMED DENMARK A/S for the gift of lornoxicam, and also the GSRT for the funding of a bilateral project, Research and Technological Co-operation Greece-Poland, and for the funding support from the research program PENED 99 ED 442. We thank the Centrum of NMR of the University of Ioannina.

[1] J. A. Balfour, A. Fitton, L. B. Barradell, *Drugs* **1996**, *51*, 639.
[2] T. P. Pruss, H. Stroissning, S. Radhofer-Welte, W. Wendtlandt, N. Mehdi, F. Takacs, H. Fellier, *Postgrad. Med. J.* **1990**, *66 (Suppl.* 4), 18.
[3] [3a] R-S. Tsai, P-A. Carrupt, N. El Tayar, Y. Giroud, P. Andrade, B. Testa, F. Brèe, J.-P. Tillement, *Helv. Chim. Acta* **1993**, *76*, 842. [3b] M. R Caira, L. R. Nassimbeni, M. Timme, *J. Pharm. Scienc.* **1995**, *84*, 884. [3c] E. Bernhard, F. Zimmermann, *Arzneim-Forsch. Drug Res.* **1984**, *34*, 647.
[4] [4a] J. J. Zuckerman (Ed.), "*Organotin Compounds: New Chemistry and Applications",* Advances in Chemistry Series, no 157, American Chemical Soc., Washington, **1976**. [4b] C. J. Evans, S. Karpel, "*Organotin Compounds in Modern Technology",* J. Organomet. Chem. Library 16, Elsevier, **1985**. [4c] S. J. Blunden, P. A. Cusack, R. Hill, "*Industrial Uses of Tin Chemicals",* Royal Society of Chemistry. London, **1985**. [4d] A. J. Crowe, in M. Gielen (Ed.), *Metal-Based Antitumour Drugs*, vol. 1, Freund, London, **1989**.
[5] [5a] M. Gielen, *Coord. Chem. Rev.* **1996**, *15*, 41. [5b] D. Kovala-Demertzi, P. Tauridou, U. Russo, M. Gielen, *Inorg. Chim. Acta* **1995**, *239*, 177. [5c] V. Dokorou, Z. Ciunik, U. Russo, D. Kovala-Demertzi, *J. Organom. Chem.* **2001**, *630*, 205. [5d] D. Kovala-Demertzi, V. Dokorou, Z. Ciunik, N. Kourkoumelis, M. A. Demertzis, *Appl. Organom. Chem.* **2002**, *16*, 360.
[6] [6a] D. Kovala-Demertzi, A. Theodorou, M. A. Demertzis, C. Raptopoulou, A. Terzis, *J. Inorg. Biochem.* **1997**, *65*, 151. [6b] A. Theodorou, M. A. Demertzis, D. Kovala-Demertzi, E. A. Lioliou, A. A. Pantazaki, D. A. Kiriakidis, *Biometals* **1999**, *12*, 67. [6c] D. Kovala-Demertzi, *J. Inorg. Biochem.* **2000**, *79*, 153.
[7] [7a] D. Kovala-Demertzi, N. Kourkoumelis, A. Koutsodimou, A. Moukarika, E. Horn, E. R. T. Tiekink, *J. Organomet. Chem.* **2001**, *620*, 194. [7b] M. A. Demertzis, S. K. Hadjikakou, D. Kovala-Demertzi, A. Koutsodimou, M. Kubicki, *Helvet. Chim. Acta* **2000**, *83*, 2787. [7c] S. K. Hadjikakou, M. A. Demertzis, J. R. Miller, D. Kovala-Demertzi, *J. Chem. Soc., Dalton Trans.* **1999**, 663.
[8] A. Addison, R. T. Nageswara, J. Reedijk, J. Van Rijn, G. C. Verschoor, *J. Chem. Soc., Dalton.* **1984**, 1349.
[9] [9a] T. Steiner, B. Lutz, J. van der Maas, A. M. M. Schreurs, J. Kroon, M. Tamm, *Chem. Commun.* **1998**, 171. [9b] T. Steiner, M. Tamm, A. Grzegorzewski, N. Schulte, N. Veldman, A. M. M. Schreurs, J. Kroon, J. van der Maas, B. Lutz, *J. Chem. Soc., Perkin Trans.* **1996**, *2*, 2441. [9c] M. C. Etter, *Acc. Chem. Res.* **1990**, *23*, 120. [9d] G. R. Desiraju, *Acc. Chem. Res.* **1991**, *24*, 290.
[10] Hyperchem, Release 6.01 for Windows, Molecular Modeling System, 2000 Hypercube, Inc.
[11] [11a] L. J. Bellamy, *The Infrared Spectra of Complex Molecules*, Chapman and Hall, London, 1975. [11b] K. Nakamoto, *Infrared and Raman Spectra of Inorganic and Coordination Compounds* 4th ed., John Wiley & Sons, New York, **1980**.
[12] [12a] C. Mealli, D. Proserpio, CACAO PC Beta-Version 5. **1998**. [12b] C. Mealli, D. Proserpio, *J. Chem. Educ.* **1990**, *11*, 440.

  

[13] [13a] D. Di Leo, F. Berrettini, R. Cini, *J. Chem. Soc., Dalton Trans.* **1998**, 1993. [13b] D. Kovala-Demertzi, N. Kourkoumelis, M. A. Demertzis, J. R. Miller, C. Frampton, D. X. West, *Eur. J. Inorg. Chem.* **2000**, 727.
[14] J-I Yoshida, K. Nishiwaki, *J. Chem. Soc., Dalton Trans.* **1998**, 2589.
[15] [15a] *CrysAlisRed v. 162*, KUMA Diffraction, Wroclaw, Poland, **2000**. [15b] R. H. Blessing, *J. Appl. Crystallogr.* **1989**, *22*, 396.
[16] [16a] G. M. Sheldrick, *Acta Crystallogr., Sect. A* **1990**, *46*, 467. [16b] G. M. Sheldrick, SHELXL-97, Program for the Refinement of Crystal Structures, University of Göttingen, Germany, **1997**.

Received September 15, 2002

  